Agricultural Water Management 232 (2020) 106044

Contents lists available at ScienceDirect

Agricultural Water Management

journal homepage: www.elsevier.com/locate/agwat

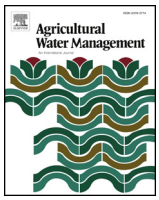

Numerical simulations of the effects furrow surface conditions and fertilizer locations have on plant nitrogen and water use in furrow irrigated systems

Keith L. Bristow[a,*], Jirka Šimůnek[b], Sarah A. Helalia[b], Altaf A. Siyal[c]

[a] CSIRO Agriculture and Food, PMB Aitkenvale, Townsville, QLD 4814, Australia
[b] Department of Environmental Sciences, University of California Riverside, Riverside, CA 92521, USA
[c] U.S.-Pakistan Center of Advanced Studies in Water, Mehran University of Engineering and Technology, Jamshoro, Pakistan

ARTICLE INFO

Keywords:
Furrow irrigation
Triggered irrigation
Transpiration
Deep drainage
Solute transport
Nitrogen leaching
Soil evaporation
HYDRUS

ABSTRACT

The HYDRUS model can be used to evaluate the effects of different soil surface treatments at the bottom of the furrow, different initial nitrogen fertilizer locations, and different furrow irrigation rates on deep drainage and solute leaching in furrow irrigated systems. This paper extends our 2012 study, in which we considered only one irrigation cycle and ignored the effects of plants. As a result of considering only one irrigation cycle, a large amount of water was used to change the water storage in the transport domain and only limited deep drainage of water and leaching of fertilizer at the bottom of the domain occurred in most scenarios investigated. To obtain a more realistic and complete picture, we have in this study considered multiple irrigation cycles to reflect actual field practices better and accounted for root water and nitrogen uptake and plant transpiration. As in our previous study, soil surface treatments at the bottom of the furrow include untreated, compacted and an impermeable membrane, and fertilizer is initially placed at one of five different locations in the furrow or the ridge. We have also evaluated (1) the effectiveness of triggering irrigation based on a pre-set soil water pressure head at a specific location in the ridge compared with prescribed irrigation at a regular time interval to supply water and nitrogen, and (2) the effects of plant water and nitrogen uptake on the furrow water balance, infiltration, soil evaporation, deep drainage, transpiration and nitrogen leaching. Our simulations show that deep drainage and nitrogen leaching can be substantially reduced by using an impermeable membrane on the bottom of the furrow and that a substantial additional reduction in leaching can be achieved by triggering irrigation rather than using a fixed time schedule. We also show that the initial location of fertilizer has a substantial effect on nitrogen uptake and leaching.

1. Introduction

About 90 % of irrigated crops across the world are irrigated using surface irrigation, including basin, border, or furrow irrigation methods (Tiercelin and Vidal, 2006). Furrow irrigation is the most commonly used method due to its simplicity of design and low capital costs (Walker and Skogerboe, 1987). However, unlike micro-irrigation methods, such as surface and subsurface drip irrigation, furrow irrigation is much less effective in delivering the required amounts of water and nitrogen directly to the plant roots. This results in large quantities of water and nitrogen being 'lost' below the crop root zone. Consequently, areas with furrow irrigation are often a major source of nitrate, resulting in pollution of groundwater systems (e.g., Artiola, 1991; Pratt and Jury, 1984). Improved management strategies that increase irrigation efficiency and reduce nitrogen losses by leaching to groundwater are therefore urgently needed for furrow irrigated crops (Bar-Yosef, 1999).

Simulation models such as HYDRUS (2D/3D) and its predecessors SWMS-2D, CHAIN-2D and HYDRUS-2D (Šimůnek et al., 2008, 2016b) have been widely used to improve the design, management, and performance of various irrigation systems, including surface and subsurface drip irrigation and furrow irrigation. Šimůnek et al. (2016b) identified more than 25 papers that used the above models to evaluate the effect of various factors on furrow irrigation systems and here we include a subset of the 25 references most relevant to this paper (Benjamin et al., 1994; Abbasi et al., 2003a,Abbasi et al., 2003b,Abbasi et al., 2003c, 2004; Rocha et al., 2006; Wöhling et al., 2004a,b, 2006; Mailhol et al., 2007; Warrick et al., 2007; Wöhling and Schmitz, 2007; Wöhling and Mailhol, 2007; Crevoisier et al., 2008; Lazarovitch et al., 2009; Siyal et al., 2012; Soroush et al., 2012; Ebrahimian et al., 2012,

* Corresponding author.
E-mail addresses: Keith.Bristow@csiro.au (K.L. Bristow), Jiri.Simunek@ucr.edu (J. Šimůnek), shela001@ucr.edu (S.A. Helalia), aasiyal.uspcasw@faculty.muet.edu.pk (A.A. Siyal).

https://doi.org/10.1016/j.agwat.2020.106044
Received 6 November 2019; Received in revised form 16 January 2020; Accepted 23 January 2020

2013a,b; Zerihun et al., 2014). These models, which simulate water flow and/or solute transport in soils, proved to be flexible and cost-effective tools for analyzing and evaluating various management/irrigation scenarios.

One of these studies was the study of Siyal et al. (2012), who evaluated the effects of different soil surface treatments at the bottom of the furrow, different initial nitrogen fertilizer locations, and different furrow irrigation rates on deep drainage and solute leaching in a furrow irrigated system. Siyal et al. (2012) assumed that the soil at the bottom of the furrow was either a) untreated; it retained its normal surface features and soil hydraulic properties, b) compacted; the soil hydraulic conductivity of the surface soil was reduced by 80 %, or c) covered with an impermeable membrane so that the bottom of the furrow was impermeable to water flow. Siyal et al. (2012) also assumed that the nitrogen fertilizer was initially located at one of 5 different locations, ranging from the bottom of the furrow to the top of the ridge.

The strength of the Siyal et al. (2012) study was that it enabled evaluation of the worst-case scenario in terms of deep drainage and nitrogen leaching in the absence of plants. The main limitation of the Siyal et al. (2012) study was that it used only one irrigation cycle and the effects of plants were neglected. Their results showed that deep drainage and nitrogen leaching were significantly affected by the initial soil moisture conditions since a large amount of water was used to change the soil water storage in the root zone (transport domain) and only limited leaching occurred in most scenarios. To obtain a more realistic and complete picture, one must consider multiple irrigation cycles to reflect actual field practices better and account for plant water and nitrogen uptake, which affect deep drainage and nitrogen leaching. The reason for applying irrigation and fertilizer is to supply plants with water and nitrogen and a full analysis should consider how much of the applied water and fertilizer can be taken up by the plants.

The furrow irrigation model of Siyal et al. (2012) was further extended by Šimůnek et al. (2016a) to consider a) processes of precipitation and evaporation as a source/loss of water from the furrow and b) different timings of fertigation with irrigation water. Šimůnek et al. (2016a) then used this extended furrow irrigation model to evaluate the effects of different soil surface treatments at the bottom of the furrow and different timings of fertigation on root water and solute uptake, deep drainage and solute leaching in a loamy soil.

To overcome the limitations of the study of Siyal et al. (2012), in this manuscript, we expand their analysis by considering a) multiple irrigation cycles during one month and b) the effects plants have on deep drainage and leaching by accounting for root water and solute uptake. This allows us to analyze how much of the applied water and nitrogen can be taken up by the plant roots, rather than be leached from the crop root zone. We also consider an irrigation strategy where irrigation is triggered when a critical soil water pressure head is reached at a specified location in the root zone (Dabach et al., 2013), rather than being provided at regular time intervals.

The objectives of this study are i) to evaluate the effectiveness of different furrow management strategies to improve supply of water to plants and to reduce water losses due to evaporation and deep drainage, ii) to evaluate the effects of different initial fertilizer locations on the supply of nitrogen to plants and leaching from the crop root zone, iii) to evaluate the effectiveness of triggered irrigations compared with prescribed irrigations to supply water and nitrogen to plants and limit leaching from the soil profile, and iv) to assess the combined effects of plant water and nitrogen uptake with different furrow management strategies and different irrigation strategies to minimize deep drainage and nitrogen leaching.

2. Material and methods

2.1. Governing equations for water flow and solute transport

The HYDRUS (2D/3D) software package (Šimůnek et al., 2008) was used to carry out computer simulations. HYDRUS uses numerical solutions of the Richards' and convection-dispersion equations for variably-saturated water flow and solute transport in soils, respectively:

$$\frac{\partial \theta}{\partial t} = \frac{\partial}{\partial x_i}\left[K\left(K_{ij}^A \frac{\partial h}{\partial x_j} + K_{iz}^A\right)\right] - S \quad (1)$$

$$\frac{\partial \theta c}{\partial t} = \frac{\partial}{\partial x_i}\left(\theta D^{ij} \frac{\partial c}{\partial x_j}\right) - \frac{\partial q_i c}{\partial x_i} - Sc_r \quad (2)$$

In Eq. 1, θ is the volumetric water content [L^3L^{-3}], h is the pressure head [L], S is a sink term accounting for plant water uptake [T^{-1}], x_i (i = 1,2) are the spatial coordinates [L], t is time [T], K_{ij}^A are components of a dimensionless anisotropy tensor $\mathbf{K}^A$, and K is the unsaturated hydraulic conductivity function [LT^{-1}] given by the product of the relative hydraulic conductivity K_r and the saturated hydraulic conductivity K_s [LT^{-1}]. In Eq. 2, c is the solute concentration [ML^{-3}], q_i is the i-th component of the volumetric flux density [LT^{-1}], D_{ij} is the dispersion coefficient tensor [L^2T^{-1}], and c_r is the concentration of the sink term [ML^{-3}]. Note that although HYDRUS (2D/3D) solves a more general solute transport equation than Eq. 2, only terms considered in this study are given here.

Numerical solution of the Richards' equation (Eq. 1) requires as input the soil hydraulic parameters describing the soil water retention curve and the hydraulic conductivity function. In this study, we use the analytical model of van Genuchten (1980) to describe these two functions. The soil hydraulic parameters for a loamy soil were taken from the soil catalog provided by the HYDRUS software and are the same as those used by Siyal et al. (2012) and Šimůnek et al. (2016a). The values of these parameters are: the residual water content = 0.078, the saturated water content = 0.43, the shape parameters α and n are 0.036 cm^{-1} and 1.56, respectively, and the saturated hydraulic conductivity = 24.96 cm/day.

2.2. Flow domain, initial and boundary conditions

The same flow domain and initial and boundary conditions, as in Siyal et al. (2012), were used in this study (Fig. 1). The transport domain was 100 cm wide and 100 cm high. The ridge was 40 cm wide. The furrow was 15 cm deep and 30 cm wide, and the side of the furrow had a slope of 45°. The initial pressure head varied linearly between -200 cm at the bottom of the domain and - 300 cm at the top of the ridge.

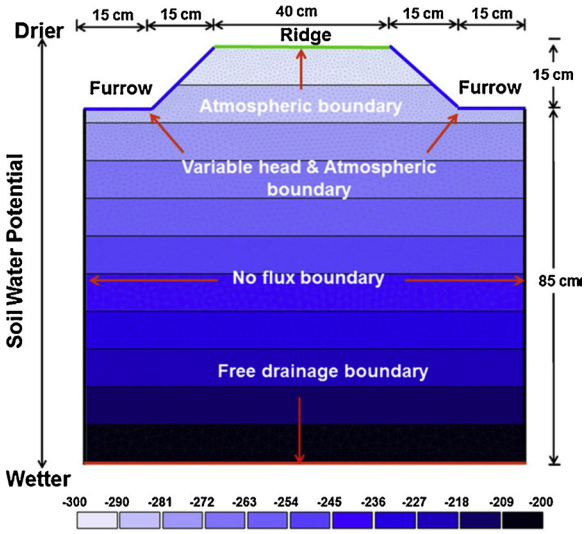

Fig. 1. Initial soil water pressure head (cm) in the flow domain and boundary conditions imposed on the flow domain during simulations (Siyal et al., 2012; with permission).

Boundary conditions imposed on the flow domain included an atmospheric boundary condition at the top of the ridge, a free drainage boundary condition at the bottom of the soil profile, a no-flow boundary condition at both vertical sides, and special boundary conditions were applied at the base of the furrow (see Section 2.4 below) to reflect the different surface conditions being investigated.

2.3. The furrow irrigation submodule

The furrow irrigation submodule, as developed in Appendix A of Siyal et al. (2012) and extended by Šimůnek et al. (2016a), was used to simulate furrow irrigation and dynamic position of the water level in the furrow during irrigation. Šimůnek et al. (2016a) extended the model of Siyal et al. (2012) by adding the atmospheric boundary condition at the water surface in the furrow and thus allowing evaporation from and precipitation to the water surface. In this submodule, the water level in the furrow is calculated from the water balance, accounting for the applied irrigation, infiltration and the change in water volume in the furrow. When water is present in the furrow, the time-variable pressure head boundary condition is applied to the furrow boundary that is below the surface water level, reflecting the dynamic nature of the water level in the furrow. An atmospheric boundary condition is applied in the furrow when it is empty of water, and above the water level in a furrow when it is not. An atmospheric boundary condition considers precipitation ($P = 0$) and potential evapotranspiration ($ET_p = E_p + T_p = 1.0$ cm/d) fluxes. Potential evapotranspiration (ET_p) equal to 1 cm/day corresponds to conditions in January in north Queensland, Australia. Note that we assume that plant leaves cover only the ridge and that the leaf area index is about 3.5, which corresponds to a surface cover fraction of about 80 %. At the top of the ridge, we assume that a fraction (80 %) of incoming energy ($ET_p = E_p + T_p = 1.0$ cm/d) is intercepted by plants (potential transpiration $T_p = 0.8$ cm/d) and the remaining fraction (20 %) by the soil surface (potential evaporation $E_p = 0.2$ cm/d). All incoming energy in the furrow reaches either the water level in the furrow (during irrigation) or the bottom of the furrow (between irrigations) ($E_p = ET_p = 1.0$ cm/d).

2.4. Soil surface management and fertilizer placement strategies

The same soil surface management and fertilizer placement strategies, as in Siyal et al. (2012), were considered in this study (see Fig. 2). It was assumed that the soil at the bottom of the furrow was either a) untreated; it retained its usual surface features and soil hydraulic properties (S_0), b) compacted; its hydraulic conductivity was reduced by 80 % while the retention parameters were considered to remain the same (S_c), or c) covered with an impermeable membrane so that the bottom of the furrow was impermeable (S_{im}). Nitrogen fertilizer was mixed into the top 1 − 3 cm of the soil a) at the bottom and center of the furrow (P_1), b) on the sides of the furrow (P_2), c) on the bottom and sides of the furrow (P_3), d) on the furrow sides near the ridge top (P_4), and e) on the top and center of the ridge (P_5) (Fig. 2).

While the HYDRUS model allows one to consider the fate and transport of multiple solutes of various properties subject to first-order degradation chain reactions, such as the nitrification chain from urea to ammonium and nitrite and nitrate (e.g., Hanson et al., 2006; Ramos et al., 2012; Li et al., 2015), only one nonreactive solute species and dimensionless concentrations were used in our simulations. The initial concentration of this nonreactive solute, which could be considered as a surrogate for nitrate readily available for transport and plant uptake, in the initial placement area was adjusted so that the initial solute mass in the soil profile was equal to 1 (100 %). This enabled us quick evaluation of the fractions of nitrogen fertilizer that were used by plants, leached from the soil root zone, and remained in the soil profile.

2.5. Irrigation strategies

Water application rates of 1200, 1400, 1600, 1800 and 2000 L h^{-1} furrow^{-1} for a 100 m long furrow, corresponding to area-based application rates of 12, 14, 16 18, and 20 mm h^{-1}, or to rates of 60, 70, 80, 90 and 100 cm^2 h^{-1} in our two-dimensional domain, respectively, were compared in this study. The switch-off depth, which determines when the supply of irrigation water is stopped was set at 10 cm (Siyal et al., 2012). Irrigation was applied every five days for 30 days. A second irrigation strategy where irrigation was triggered (Dabach et al., 2013, 2015) when the soil water pressure head in the middle of the ridge and 15 cm below the top of the ridge reached a pre-set value of -500 cm was also included for comparative purposes. An optimal location of the triggering point and an optimal triggering pressure head for different plants and soil types is a topic of ongoing research (Dabach et al., 2013, 2015). Note that this triggering point is located in the middle of the root zone with the highest root density (see Fig. 3 below). According to the stress response function described in the next Section, irrigation is triggered when root water uptake is reduced by about 4 %.

2.6. Root water and nitrogen uptake

The approach of Feddes et al. (1978) was used to describe plant water uptake:

$$S(h) = \alpha(h) b(x, z) L_t T_p \tag{3}$$

where S is defined as the volume of water removed per unit time from a unit volume of soil due to root water uptake [T^{-1}], $\alpha(h)$ is a prescribed dimensionless water stress response function of the soil water pressure head ($0 \le \alpha \le 1$), $b(x, z)$ is the normalized water uptake distribution function [L^{-2}], L_t is the width [L] of the soil surface associated with the transpiration process ($L_t = 40$ cm; surface of the furrow ridge, see the definition of the transport domain below), and T_p is the potential transpiration rate [LT^{-1}] ($T_p = 0.8$ cm/d). Water uptake is assumed to be zero close to saturation (above h_1) and when the soil is dry (for $h < h_4$, the wilting point pressure head). Water uptake is considered optimal between pressure heads h_2 and h_3, whereas for pressure heads between h_3 and h_4 (or h_1 and h_2), water uptake decreases (or increases) linearly with h (Feddes et al., 1978). The following parameters of the stress response function (typical for many crops) were used in our study: $h_1 = -10$ cm, $h_2 = -25$ cm, $h_3 = -200$ cm, and $h_4 = -8000$ cm.

The spatial distribution of roots of a hypothetical plant is described using the two-dimensional root distribution function $b(x,z)$ of Vrugt et al. (2001, 2002):

$$b(x, z) = \left(1 - \frac{z}{Z_m}\right)\left(1 - \frac{x}{X_m}\right) e^{-\left(\frac{p_z}{Z_m}|z^* - z| + \frac{p_x}{X_m}|x^* - x|\right)} \tag{4}$$

where X_m and Z_m are the maximum rooting lengths in the x- and z-directions [L], respectively; x and z are distances from the origin of the plant in the x- and z-directions [L], respectively; and p_x [-], p_z [-], x^* [L], and z^* [L] are empirical parameters. The plant was assumed to be centered in the middle of the ridge; the extent of roots in the vertical (Z_m) and horizontal (X_m) direction was 60 and 35 cm, respectively; parameters x^* and z^* (sometimes referred to as *Depth and Radius of Maximum Intensity*) were 30 and 20 cm, respectively; and parameters p_x and p_z were set at one (1). These parameters produced the root distribution function presented in Fig. 3.

Only passive root nitrogen uptake was considered (Šimůnek and Hopmans, 2009), i.e., c_r in Eq. (2) was assumed to be equal to the nitrogen concentration at any particular location. No compensation mechanisms that would increase root uptake in one part (unstressed) of the root zone in response to reduced uptake in another part (stressed) of the root zone were considered in our study.

In the simulations carried out in this study, it is assumed that the parameters required to simulate root water and nitrogen uptake, i.e.,

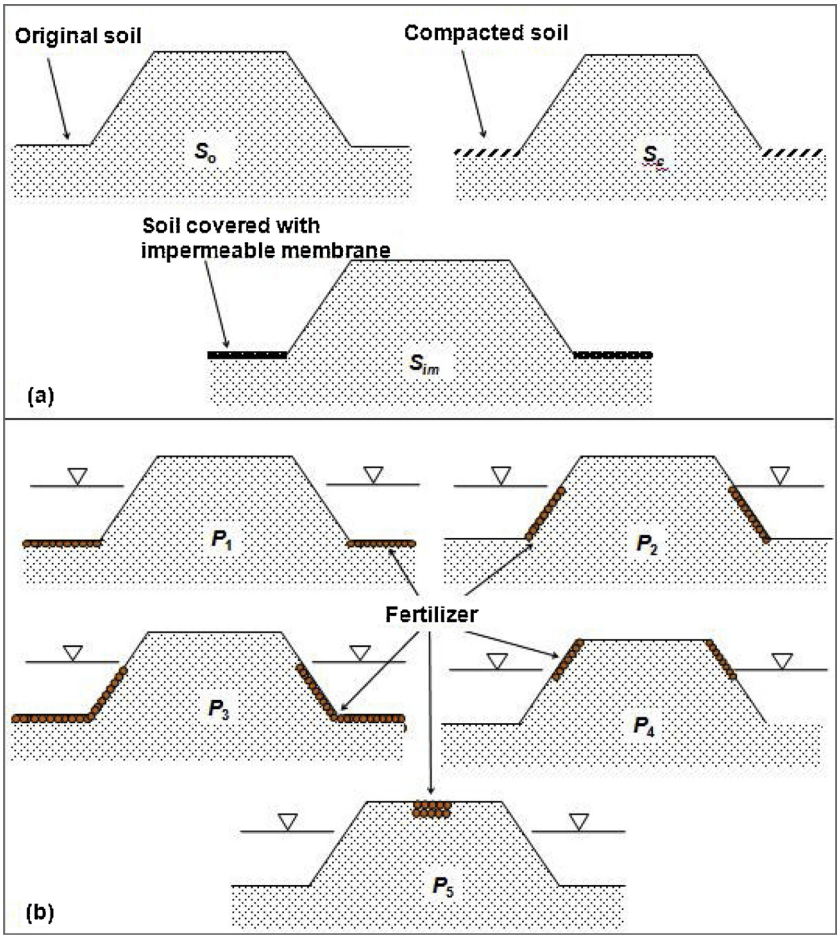

Fig. 2. Schematic showing (a) the different soil surface management treatments (S_i) and (b) fertilizer placements (P_n) analyzed in this study (S_0 - original soil; S_c - compacted soil; S_{im} – impermeable membrane, and P_1 - fertilizer at the bottom of furrow; P_2 - fertilizer on the sides of furrow; P_3 - fertilizer on the bottom and sides of the furrow; P_4 - fertilizer on the furrow sides near the ridge top; P_5 - fertilizer on the top at the center of the ridge).

the spatial root distribution, the water stress response function, and potential transpiration are constant in time. Potential root water uptake and its spatial distribution are thus static. The actual root water and nitrogen uptake and their spatial distributions are however dynamic as a result of temporal and spatial variable distributions of water content and nitrogen concentration in response to individual irrigation events. Actual transpiration and nitrogen uptake will, therefore, differ between different scenarios.

3. Results and discussion

The Results section is organized as follows. The first Section (3.1) deals with water balance in the furrow. The difference between constant incoming irrigation (during irrigation events) and time-variable infiltration produces time-variable water levels in the furrow, which are discussed in this section. Water fluxes associated with the subsurface are described next. In Section 3.2, we discuss infiltration, which is an input into the soil profile. Water losses in terms of evaporation and deep drainage are discussed in Sections 3.3 and 3.4, respectively. Next, in Section 3.5, we discuss the productive use of water, i.e., transpiration, root water uptake, and irrigation water use efficiency (defined here as a ratio of transpiration/irrigation). The change in water storage in the subsurface, a component that closes the subsurface water balance, is discussed in section 3.6. Finally, components of the nitrogen balance, including nitrogen leaching, plant nitrogen uptake and nitrogen storage in the crop root zone, are discussed in the last Section (3.7).

3.1. Furrow water balance

The total amount of irrigation water applied during one irrigation cycle depends on several factors, including soil surface management, which affects the infiltration rate, and the applied irrigation rate. Fig. 4 shows water levels in the furrow for the three different soil surface conditions, i.e., S_0, S_c, and S_{im} for 5 different irrigation rates. Fig. 5 shows cumulative irrigation and infiltration fluxes for the first scenario (S_0) and different fluxes. Similar graphs could be produced for the other two soil surface conditions. Fig. 4 shows that the switch-off depth is reached fastest for the S_{im} treatment with an impermeable bottom and slowest for the S_0 treatment with the standard untreated bottom. It also shows that the switch-off depth is reached faster for larger irrigation rates.

Figs. 4 and 5 indicate that most water is applied, in each treatment, when the lowest irrigation rate is used. This is because when water is applied at a lower rate it is applied during a longer time period. Since infiltration rates are relatively similar (Fig. 5, right), the lowest irrigation rate produces the slowest increase in the water level in the furrow, reaching the switch-off depth much slower than the higher irrigation rates. Consequently, irrigation water for smaller irrigation rates is applied longer, resulting in more water being applied (Fig. 5, left).

Fig. 6 shows water levels in the furrow for the three soil surface treatments, i.e., S_0, S_c, and S_{im}, for five different irrigation rates when irrigations are triggered by the soil water status in the root zone. This figure shows that irrigations are triggered less often for lower irrigation rates, which, as explained above, provide larger amounts of applied water. Since larger amounts of water are applied when lower irrigation

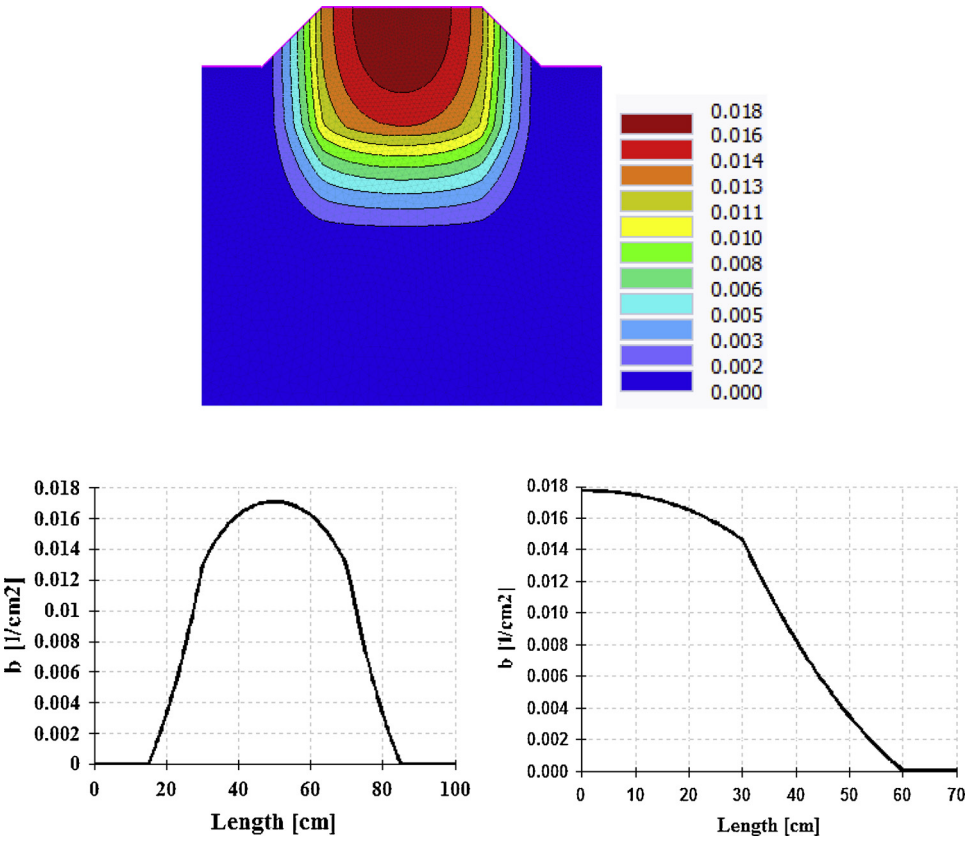

Fig. 3. Spatial root distribution function $b(x,z)$ (top). The bottom left is $b(x,z)$ along the soil surface and the bottom right is $b(x,z)$ along the vertical cross-section through the middle of the domain.

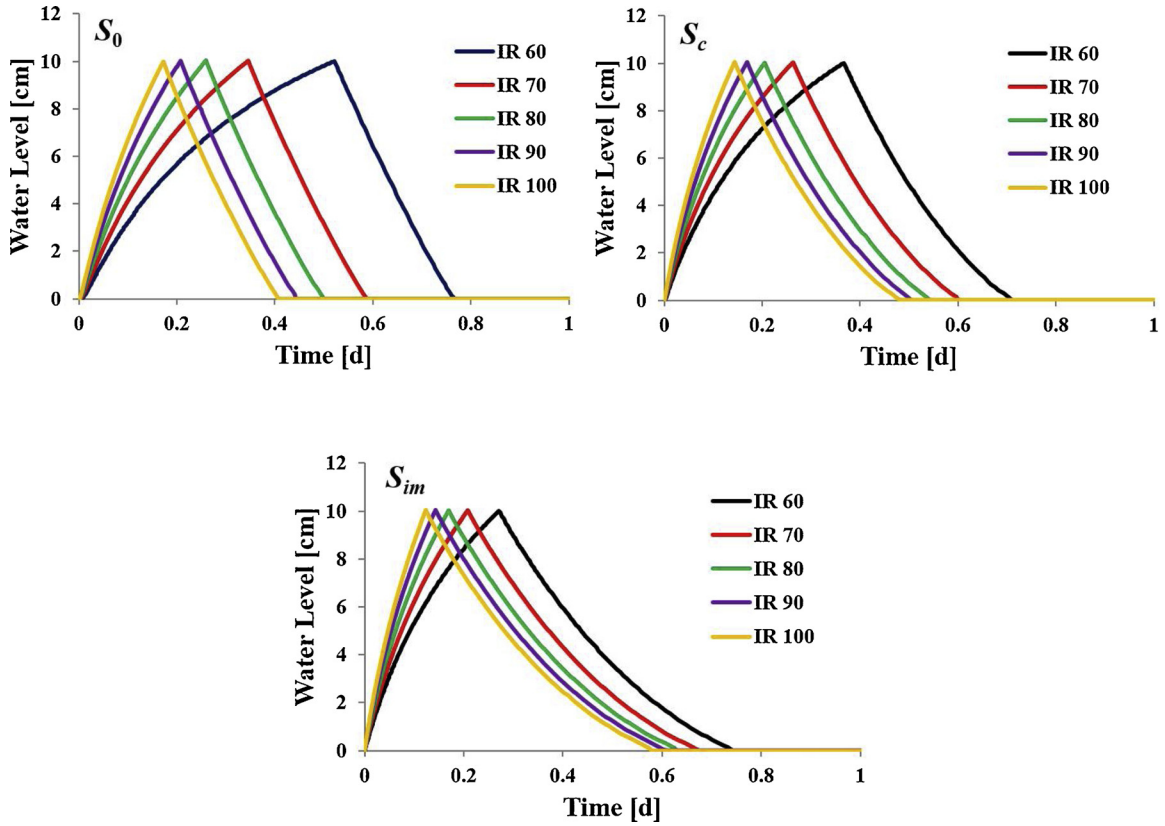

Fig. 4. Water levels in the furrow for the different soil surface conditions S_0 (top left), S_c (top right), and S_{im} (bottom) for irrigation rates (IR) of 60 (IR 60), 70 (IR 70), 80 (IR 80), 90 (IR 90), and 100 (IR 100) $cm^2\ h^{-1}$.

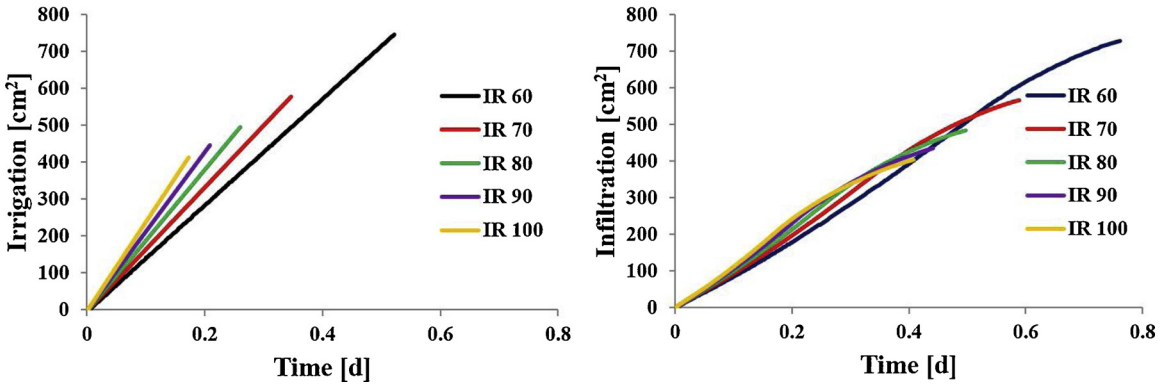

Fig. 5. Cumulative irrigation (left) and infiltration (right) for treatments S_0 and for irrigation rates (IR) of 60 (IR 60), 70 (IR 70), 80 (IR 80), 90 (IR 90), and 100 (IR 100) cm^2 h^{-1}.

rates are used, it takes longer for this water to be 'used' by plants, soil evaporation, and deep drainage. This figure also shows that irrigations are triggered later for treatment S_0 than for treatments S_c and S_{im}. This is again because more water is applied to treatment S_0 in each irrigation cycle.

It should also be emphasized that four irrigation events were triggered for IR 80, IR 90, and IR 100 for all surface treatments. On the other hand, for IR 70, four irrigation events were triggered only for treatments S_c and S_{im}, while only 3 irrigation events were triggered for treatment S_0. Finally, for IR 60, only three irrigation events were triggered for treatments S_0 and S_c, while four irrigation events were triggered for treatment S_{im}. However, this irrigation event was not completed during the 30-d simulation. This factor, i.e., a different number of irrigation events for triggered irrigation scenarios, can explain some of the nonlinearities and unexpected results discussed below.

3.2. Infiltration

Fig. 7 shows cumulative infiltration during one month (30 days) expressed in absolute values (Fig. 7, top) and as a percentage of potential evapotranspiration (Fig. 7, bottom). Cumulative potential evapotranspiration ET_p is equal to 3000 cm^2 (i.e., 1 cm/d * 30 d *100 cm = 3000 cm^2). Cumulative infiltration is displayed for different surface treatments, different irrigation rates, and irrigations applied at regular intervals or triggered by soil water status in the ridge.

Total infiltration decreases with an increasing irrigation rate. When the irrigation rate is low, it takes much longer before the switch-off depth is reached, during which time the water infiltrates into the soil profile (see Fig. 4). When the bottom of the furrow is compacted or impervious, the switch-off depth is reached much faster, and less water is applied. This is true for irrigation applied at a regular interval of 5 days or triggered by soil water conditions in the ridge. The differences between different furrow surface treatments are much smaller when "triggered" irrigations are applied since, in this case, the soil profile

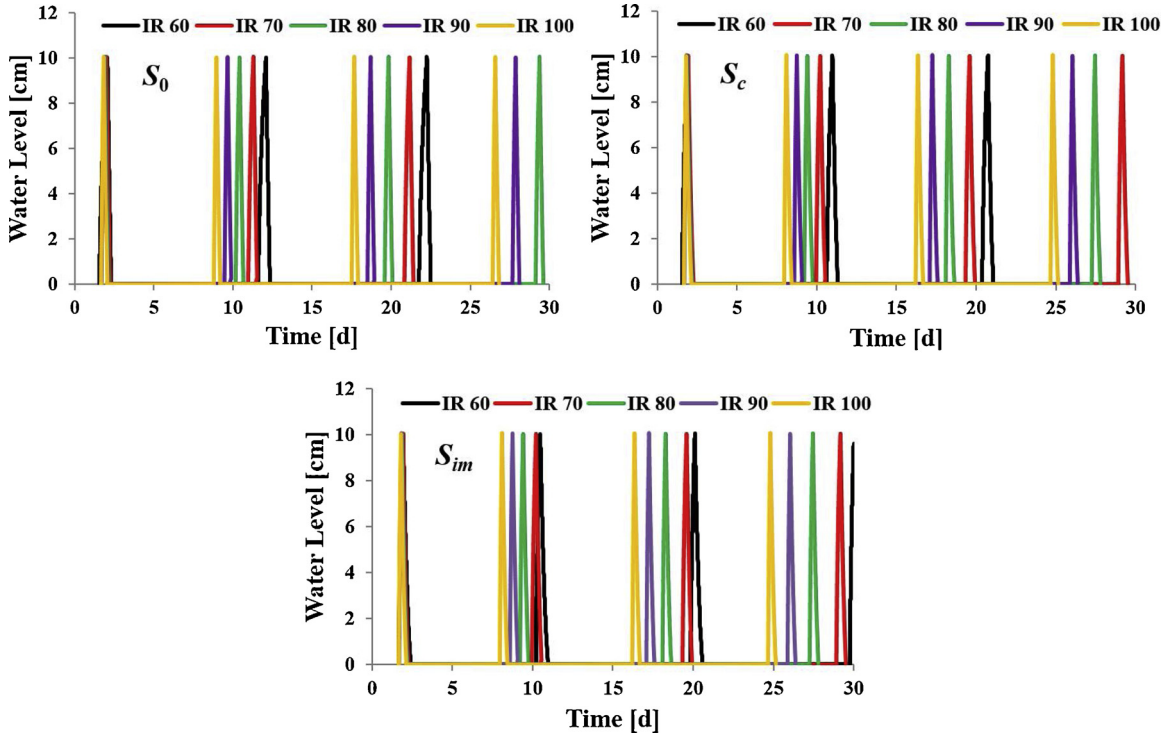

Fig. 6. Water levels in the furrow for soil surface treatments S_0 (top left), S_c (top right), and S_{im} (bottom) for irrigation rates (IR) of 60 (IR 60), 70 (IR 70), 80 (IR 80), 90 (IR 90), and 100 (IR 100) cm^2 h^{-1} for triggered irrigations.

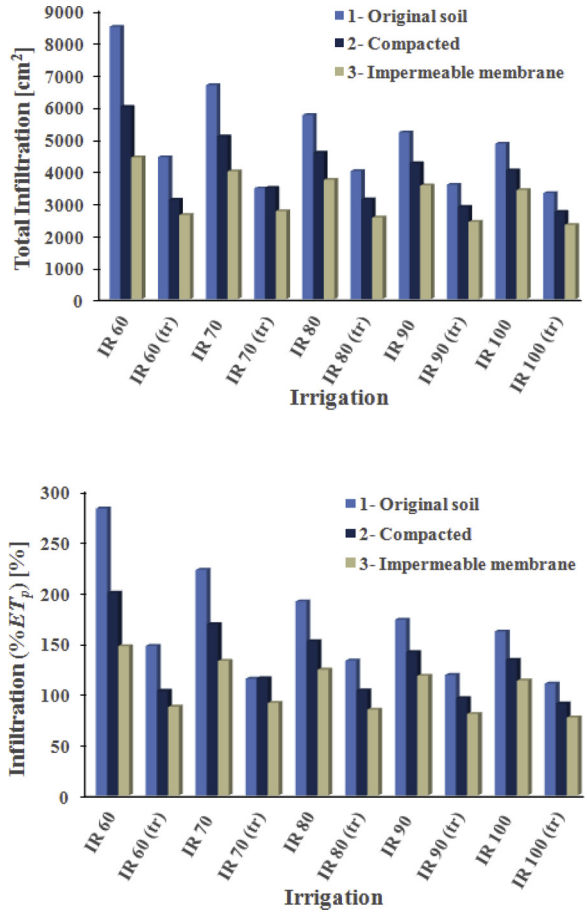

Fig. 7. Cumulative infiltration (top - expressed in absolute values, bottom - expressed as a percentage of potential evapotranspiration) as a function of the surface treatment (S_0 - original, S_c - compacted, and S_{im} - impermeable membrane), for irrigation rates (IR) of 60 (IR 60), 70 (IR 70), 80 (IR 80), 90 (IR 90), and 100 (IR 100) cm^2 h^{-1}, and irrigations applied at regular intervals or triggered (tr).

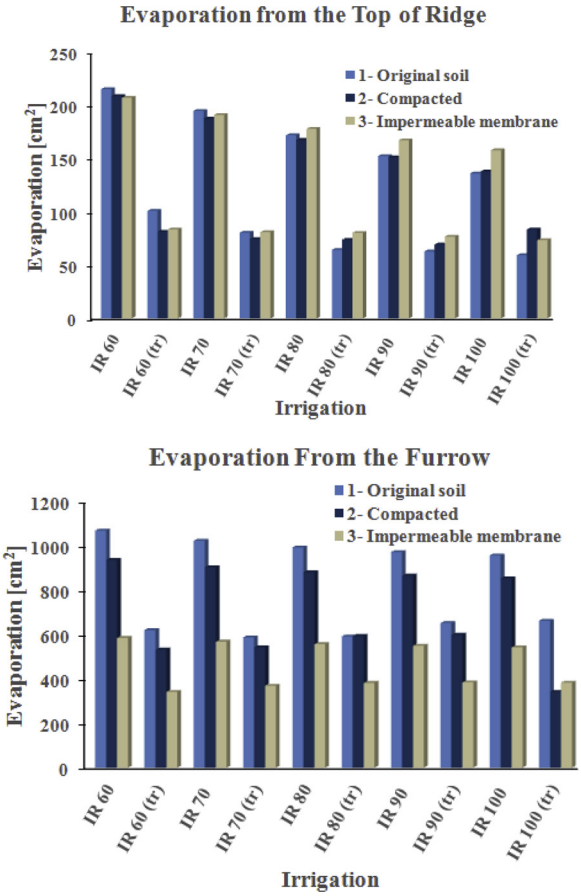

Fig. 8. Evaporation from the top of the ridge (top) and the furrow (bottom) as a function of surface treatment (S_0 - original, S_c - compacted, and S_{im} - impermeable membrane), for irrigation rates (IR) of 60 (IR 60), 70 (IR 70), 80 (IR 80), 90 (IR 90), and 100 (IR 100) cm^2 h^{-1}, and irrigations applied at regular intervals and triggered (tr).

controls how many irrigations are applied and at what time (see Fig. 6).

Fig. 7, which shows cumulative infiltration as a fraction of cumulative potential evapotranspiration (ET_p), indicates that triggered irrigation keeps the amount of applied water close to 100 % ET_p (or even below for the impermeable or compacted bottom of the furrow). Interestingly, there were only small differences between applied irrigation volumes when irrigation was triggered by conditions in the soil and flow through the bottom of the furrow was restricted, contrary to standard irrigation when irrigation volumes substantially increased with the decrease of the irrigation rate. For normal conditions, one would need to use either a lower switch-off depth or a longer time interval between irrigations to get closer to 100 % ET_p and to avoid significant leaching losses.

3.3. Evaporation

Fig. 8 shows cumulative evaporation fluxes from the top of the ridge and the furrow during one month (30 days) for different surface treatments, different irrigation rates, and irrigations applied at regular intervals or triggered by soil water status in the Ridge. Cumulative actual evaporation from the top of the ridge (Fig. 8, top) can be compared with cumulative potential evaporation, which is equal to 240 cm^2 (E_p = 0.2 cm/d; cum(E_p) = 0.2 cm/d * 40 cm * 30 d = 240 cm^2). Note that we set potential evaporation at 0.2 cm/d at the top of the ridge because the remaining incoming energy is intercepted by the plant (T_p = 0.8 cm/d). Also note that for triggered irrigations, evaporation losses are substantially reduced (less than 50 % of potential E_p) compared to irrigations at predetermined intervals. In general, evaporation losses for triggered irrigation are less than half of those for irrigations at predetermined intervals. Also, note that evaporation losses are more or less independent of the soil surface treatment.

Cumulative evaporation from the furrow bottom and sides (Fig. 8; bottom) can be compared with potential evaporation, which is approximately equal to 1800 cm^2 (E_p = 1.0 cm/d; cum(E_p) = 1.0 cm/d * 60 cm * 30 d = 1800 cm^2; note that this formula should exclude time (about 1 d) when the furrow bottom is flooded with water and evaporation does not occur directly from the furrow bottom). Cumulative potential evaporation for the S_{im} treatment is 900 cm^2 (E_p = 1.0 cm/d * 30 cm * 30 d = 900 cm^2). For the furrow, we assume that all incoming energy is converted to potential evaporation (E_p = 1.0 cm/d). Note again that evaporation losses from the furrow are substantially reduced when we used triggered irrigation compared to irrigation at prescribed intervals. Evaporation losses from the furrow are lowest for the treatment with the impermeable membrane since, in this case, water can evaporate only from the sides of the furrow.

3.4. Deep drainage

Fig. 9 shows drainage at the bottom of the soil profile during one month (30 days) for different furrow surface treatments and different irrigation rates, and irrigations applied at prescribed regular intervals or triggered by the soil water status in the ridge. The drainage loss reflects the amount of irrigation water applied in the different

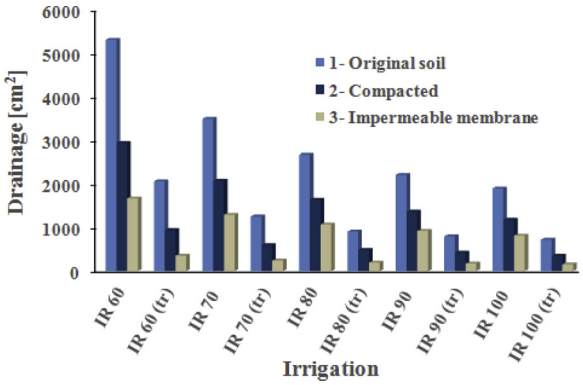

Fig. 9. Drainage losses from the soil profile as a function of the furrow surface treatment (S_0 - original, S_c - compacted, and S_{im} - impermeable membrane), for irrigation rates (IR) of 60 (IR 60), 70 (IR 70), 80 (IR 80), 90 (IR 90), and 100 (IR 100) cm^2 h^{-1}, and irrigations applied at regular intervals and triggered (tr).

treatments. The largest drainage loss occurred in the treatment with standard soil surface features and soil hydraulic properties, with lower applied rates of irrigation, and for irrigations applied at a regular time interval. Drainage losses are dramatically reduced when the bottom of the furrow is covered with an impermeable membrane, and even more so when irrigations are triggered according to the preset soil water status in the ridge. It must be emphasized that triggered irrigations, especially in the treatment with the impermeable membrane on the base of the furrow, can practically eliminate drainage losses.

3.5. Transpiration

The ultimate goal of irrigation is to supply crops with the right amount of water, at the right place and at the right time to maximize plant transpiration, and hence crop yield. Fig. 10 shows the cumulative actual transpiration as an absolute value. Cumulative potential transpiration is 960 cm^2 (T_p = 0.8 cm/d, and cum(T_p) = 0.8 cm/d * 40 cm * 30 d = 960 cm^2) during one month (30 days) irrespective of different surface treatments, different irrigation rates, and irrigations applied at a regular interval or triggered by a pre-set condition (soil water pressure head) in the ridge. Cumulative transpiration is large for all scenarios (more than 90 % of potential transpiration). However, cumulative transpiration values are smaller (by about 6 %) for scenarios with triggered irrigation, likely because of less irrigation water applied in these scenarios (Fig. 7). Since the loss in crop yield is often assumed to be directly correlated with the ratio of cumulative actual and potential

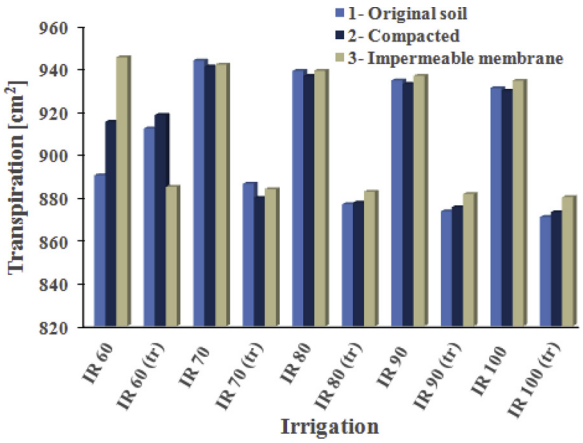

Fig. 10. Total transpiration as a function of the furrow surface treatment (S_0 - original, S_c - compacted, S_{im} - impermeable membrane), for irrigation rates (IR) of 60 (IR 60), 70 (IR 70), 80 (IR 80), 90 (IR 90), and 100 (IR 100) cm^2 h^{-1}, and irrigations applied at regular intervals and triggered (tr).

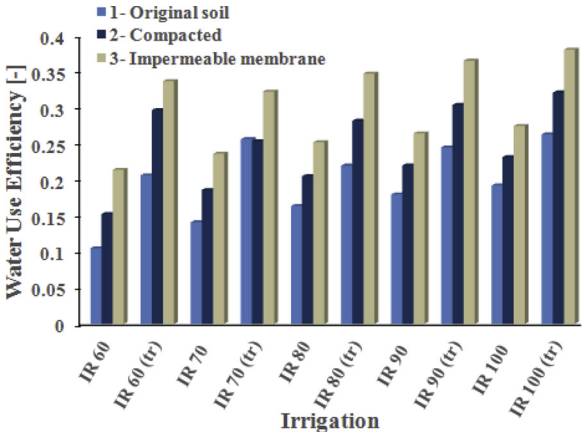

Fig. 11. Irrigation water use efficiency as a function of surface treatment scenario (S_0 - original, S_c - compacted, and S_{im} - impermeable membrane), for irrigation rates (IR) of 60 (IR 60), 70 (IR 70), 80 (IR 80), 90 (IR 90), and 100 (IR 100) cm^2 h^{-1}, and irrigations applied at regular intervals and triggered (tr).

transpirations (e.g., Klocke et al., 2004; Payero et al., 2006; Oster et al., 2012; Ragab et al., 2015), the scenarios with triggered irrigation will thus likely lead to a slight loss of crop yield (on average by about 6 %). Scenarios with the impermeable membrane almost always show similar plant transpiration as the other soil surface treatments. However, this is achieved with much less water.

Fig. 11 shows the irrigation water use efficiency (WUE) for the different surface treatments, different irrigation rates, and irrigations applied at regular intervals or triggered by soil water status in the ridge. We define irrigation water use efficiency as the ratio of actual transpiration to the amount of applied irrigation water. WUE is always substantially higher for treatments with a reduced conductivity at the bottom of the furrow. It is also markedly higher for the treatment with an impermeable membrane compared with the compacted soil treatment. In general, scenarios with triggered irrigations have higher WUE than scenarios with irrigation at a regular time interval. However, this increase in WUE for scenarios with triggered irrigation is accompanied by a slight decrease in actual transpiration (Fig. 10), and correspondingly in crop yield.

Relatively low WUEs, even for triggered irrigation, which have been shown to almost eliminate downward leaching, are due to relatively large evaporation losses from the furrow and an increase in water storage in the soil profile. While furrow irrigation efficiencies, which can range from about 30 % (Fahong et al., 2004) up to about 65 % (Arabiyat et al., 1999), are in general much lower than well managed subsurface drip irrigation systems (Ayars et al., 1999), furrow irrigation remains considerably cheaper than drip systems and thus widely used around the world. Note that in our simulations potential transpiration (0.8 cm/d (T_p) * 40 cm (ridge width) = 32 cm^2/d) is only about 30% of the incoming energy (1.0 cm/d (ET_p) *100 cm (surface with) = 100 cm^2/d), and WUE of 40% is a relatively good outcome for these conditions.

3.6. Change in water storage

The change in water storage in the soil profile (Fig. 12) was similar for all scenarios with prescribed irrigation (i.e., triggered). While the initial soil water storage was about 1690 cm^2, which reflected the average soil water content of about 0.18 cm^3 cm^{-3}, the pseudo-steady-state (i.e., the same saturation conditions were obtained at the end of each irrigation cycle) was reached after 2 irrigation cycles, with the average water storage of about 2660 cm^2, which reflected the average soil water content of about 0.28 cm^3 cm^{-3}. There were only small differences between different furrow surface treatments and different irrigation rates. Similar results were also obtained for a system with

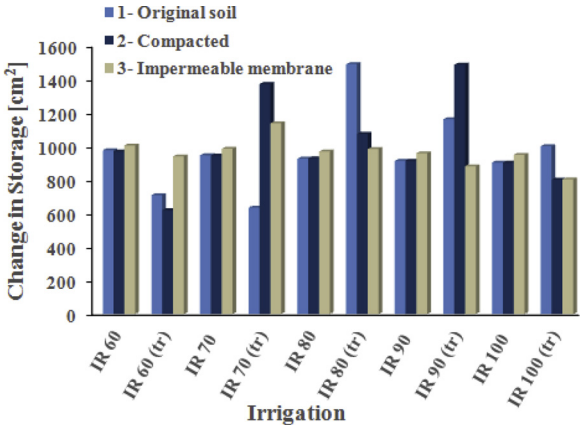

Fig. 12. The change in storage in the soil profile as a function of the surface treatment scenario (S_0 - original, S_c - compacted, and S_{im} - impermeable membrane), for irrigation rates (IR) of 60 (IR 60), 70 (IR 70), 80 (IR 80), 90 (IR 90), and 100 (IR 100) cm^2 h^{-1}, and irrigations applied at regular intervals and triggered (tr).

triggered irrigations and an impermeable membrane at the bottom of the furrow. Larger differences were only observed for systems with triggered irrigation and with original or compacted soil at the bottom of the furrow.

3.7. Nitrogen leaching, plant nitrogen uptake and nitrogen storage

While simulations evaluating water balance components were carried out for six different irrigation rates (i.e., 60, 70, 80, 90, and 100 cm^2 h^{-1} applied either at a constant time interval of 5 days or triggered by conditions in the soil), simulations evaluating solute balance components were carried out for five different initial solute placements but only one irrigation rate (again at either a prescribed regular time interval of 5 days or triggered by the soil water status in the ridge) of 90 cm^2/d (scenarios IR90 and IR90-tr, discussed above). The same irrigation rate was used as the base case in the study of Siyal et al. (2012).

Solute leaching decreased substantially with the decrease in permeability of the bottom of the furrow, from untreated, to compacted, to impermeable (Fig. 13). As expected, leaching was largest when the nitrogen fertilizer was applied at the base, base and sides, and sides of the furrow. Leaching was minimal when fertilizer was applied at the top of the ridge. These numerical results are in agreement with

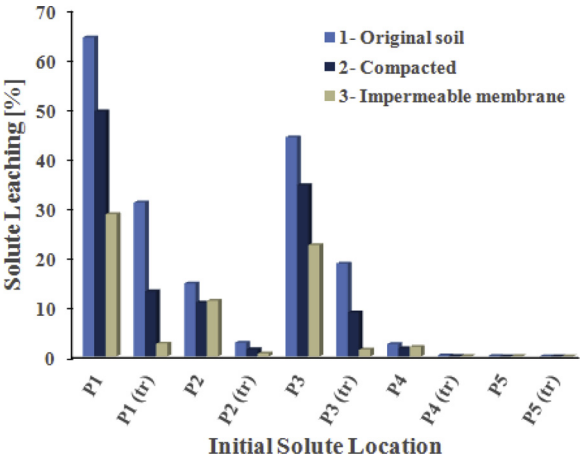

Fig. 13. Solute leaching as a function of the initial placement of fertilizer (P_1 - base, P_2- sides, P_3 - base and sides, P_4 - sides near ridge, P_5 - top of ridge); surface treatment (S_0 - original, S_c - compacted, and S_{im} - impermeable membrane); and for irrigations applied at regular intervals and triggered (tr). The irrigation rate is 90 cm^2 h^{-1}.

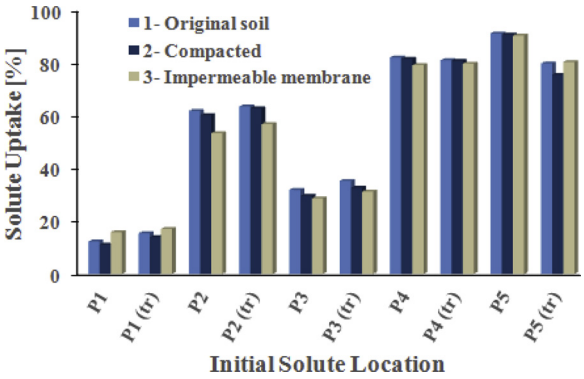

Fig. 14. Plant nitrogen uptake as a function of the initial placement of fertilizer (P_1 - base, P_2 - sides, P_3 - base and sides, P_4 - sides near ridge, P_5 - top of ridge), the surface treatment scenario (S_0 - original, S_c - compacted, and S_{im} - impermeable membrane), and for irrigation applied at regular intervals and triggered (tr). The irrigation rate is 90 cm^2 h^{-1}.

experimental studies of Kemper et al. (1975), Hamlett et al. (1990), Clay et al. (1992), Mailhol et al. (2001), and Waddell and Weil (2006) who all reported that placing fertilizer near the top of the ridge has a beneficial impact on both yield (its increase) and nitrogen leaching (its decrease). Leaching also substantially decreased when irrigations were triggered by the soil water status in the ridge, rather than prescribed at a regular time interval.

Fig. 14 shows plant nitrogen uptake as a function of the initial placement of fertilizer, surface treatment, and irrigation applied at regular intervals and triggered by the soil water status in the ridge. The irrigation rate is 90 cm^2 h^{-1}. The initial location of the fertilizer exerts a major control on plant nitrogen uptake. There is substantial nitrogen uptake when the fertilizer is placed at the top of the ridge (either in the center (about 90 % of fertilizer is taken up by roots) or on the sides (about 80 %) of the ridge). There is less uptake of nitrogen (about 60 %) when the fertilizer is placed at the sides of the furrow. Much lower uptake (10–30 %) occurs when the fertilizer is placed at the bottom of the furrow, as most of it is leached (Fig. 13). When the fertilizer is initially placed at the bottom of the furrow, it is mostly out of reach of plants and is mainly leached. There are only relatively small differences in plant nitrogen uptake as a function of the soil surface treatment at the bottom of the furrow and when irrigations are triggered or applied at a regular time interval.

Fig. 15 shows the final solute storage in the soil profile as a function of the initial placement of fertilizer, surface treatment, and for

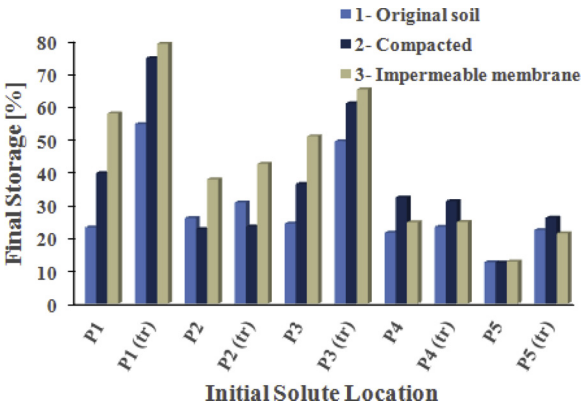

Fig. 15. Final solute storage as a function of the initial placement of fertilizer (P_1 - base, P_2 - sides, P_3 - base and sides, P_4 - sides near ridge, P_5 - top of ridge), surface treatment (S_0 - original, S_c - compacted, and S_{im} - impermeable membrane), and for irrigations applied at regular intervals and triggered (tr). The irrigation rate is 90 cm^2 h^{-1}.

irrigations applied at regular intervals and triggered with the irrigation rate of 90 $cm^2\ h^{-1}$. The final fertilizer storage in the soil profile is (more or less) inversely proportional to the fertilizer leaching. Although the plant nitrogen uptake (Fig. 14) was more or less independent of the surface treatment of the soil at the bottom of the furrow or whether irrigations were triggered or applied at a regular time interval, more fertilizer remained in the soil profile with the decrease in permeability of the bottom of the furrow, and would potentially be available for future uptake rather than leached, especially when the fertilizer was initially placed at (or close to) the bottom of the furrow. Smaller differences in solute storage were recorded between different surface treatments when the fertilizer was initially placed at the top of the ridge.

4. Conclusions

In this study, we extended the original analysis of Siyal et al. (2012) by including multiple irrigation cycles, improved irrigation scheduling based on the soil water status and root water and nutrient uptake to obtain a more realistic and complete picture of the overall water and nitrogen balance in furrow irrigated systems.

Our simulations have shown that drainage from the root zone can be substantially reduced by modifying the soil surface properties of the bottom of the furrow. When the bottom of the furrow was compacted, drainage was reduced by almost half. A further large reduction in drainage could be achieved by using an impermeable membrane on the base of the furrow. An additional and substantial decrease in drainage can be achieved using triggered irrigation based on a pre-set soil water status in the ridge. Using triggered irrigation can additionally also substantially reduce water losses through soil evaporation from both the top of the ridge and the sides and bottom of the furrow by about 50 % or more. This reduction in water loss by drainage and soil evaporation is accompanied by a relatively small decrease in transpiration (from about 98 % to about 92 %) compared with irrigation applied at a prescribed time interval. The reduction in transpiration and water loss associated with triggered irrigation is accompanied by a substantial increase in irrigation water use efficiency. Overall, our simulations indicate that significant savings of irrigation water and reduction in deep percolation and leaching can be achieved by modifying the soil surface properties of the bottom of the furrow.

Solute leaching is driven by deep drainage from the crop root zone. Substantial amounts of nitrogen are leached when the fertilizer is initially placed at the bottom of the furrow but can be greatly reduced by modifying the soil surface properties of the bottom of the furrow. When fertilizer is applied to the sides of the furrow or at the top of the ridge, nitrogen leaching is essentially eliminated, with about 60%–80% of the nitrogen being taken up by the plant. There are negligible differences in nitrogen uptake between the different soil surface treatments. Differences in root nitrogen uptake are mainly determined by the initial placement of the fertilizer.

The HYDRUS (2D/3D) model coupled with the "furrow module" proved to be a powerful tool for analyzing water flow and solute transport processes in the crop root zone in furrow irrigation and in evaluating various factors affecting this system; including irrigation rates, soil hydraulic properties at the base of the furrow and root water and nitrogen uptake. It must, however, be emphasized that this model considers processes only in two dimensions perpendicular to the actual furrow. It cannot account for flow in the third dimension, such as the advance or recession of irrigation water in the furrow. Nor can it account for the actual mixing of nitrogen with water in the furrow. The development of a pseudo-three-dimensional model that accounts for water flow down the furrow and all subsurface soil processes discussed above is currently under development (Brunetti et al., 2018; Liu et al., 2019).

It should further be emphasized that the presented simulations were carried out for a single hypothetical soil, plant, fertilizer, and weather scenario. Since several governing equations describing this system (e.g., the Richards equation or plant stress response functions) are nonlinear, obtained results cannot be directly transferred to other systems with different soils, plants, fertilizers, and weather scenarios. The simulation results discussed in this manuscript only present expected trends that would have to be confirmed by similar numerical simulations for these different conditions.

Declaration of Competing Interest

The authors declare that they have no known competing financial interests or personal relationships that could have appeared to influence the work reported in this paper.

Acknowledgments

We thank the Commonwealth Scientific and Industrial Research Organisation (CSIRO), Canberra, Australia, for supporting Professor Jirka Šimůnek's visit to Townsville, Australia, to initiate this study.

Appendix A. Supplementary data

Supplementary material related to this article can be found, in the online version, at doi:https://doi.org/10.1016/j.agwat.2020.106044.

References

Abbasi, F., Jacques, D., Šimůnek, J., Feyen, J., van Genuchten, M.T., 2003b. Inverse estimation of the soil hydraulic and solute transport parameters from transient field experiments: heterogeneous soil. Trans. ASAE 46 (4), 1097–1111.

Abbasi, F., Feyen, J., van Genuchten, M.T., 2004. Two-dimensional simulation of water flow and solute transport below furrows: model calibration and validation. J. Hydrol. 290 (1–2), 63–79.

Abbasi, F., Šimůnek, J., Feyen, J., van Genuchten, M.T., Shouse, P.J., 2003a. Simultaneous inverse estimation of soil hydraulic and solute transport parameters from transient field experiments: homogeneous soil. Trans. ASAE 46 (4), 1085–1095.

Abbasi, F., Šimůnek, J., van Genuchten, M.T., Feyen, J., Adamsen, F.J., Hunsaker, D.J., Strelkoff, T.S., Shouse, P.J., 2003c. Overland water flow and solute transport: model development and field-data analysis. J. Irrig. Drainage Eng. 129 (2), 71–81.

Artiola, J.F., 1991. Non-uniform leaching of nitrate and other solutes in a furrow-irrigated, sludge amended field. Commun. Soil Sci. Plant Anal. 22, 1013–1030.

Bar-Yosef, B., 1999. Advances in fertigation. Adv. Agron. 65, 1–75.

Benjamin, J.G., Havis, H.R., Ahuja, L.R., Alonso, C.V., 1994. Leaching and water flow patterns in every-furrow and alternate-furrow irrigation. Soil Sci. Soc. Am. J. 58 (5), 1511–1517.

Brunetti, G., Šimůnek, J., Bautista, E., 2018. A hybrid finite volume-finite element model for the numerical analysis of furrow irrigation and fertigation. Comput. Electron. Agric. 150, 312–327. https://doi.org/10.1016/j.compag.2018.05.013.

Clay, S.A., Clay, D.E., Koskinen, W.C., Malzer, G.L., 1992. Agrichemical placement impacts on alachlor and nitrate movement through soil in a ridge tillage system. J. Environ. Sci. Health B 27, 125–138.

Crevoisier, D., Popova, Z., Mailhol, J.C., Ruelle, P., 2008. Assessment and simulation of water and nitrogen transfer under furrow irrigation. Agric. Water Manag. 95 (4), 354–366.

Dabach, S., Lazarovitch, N., Šimůnek, J., Shani, U., 2013. Numerical investigation of irrigation scheduling based on soil water status. Irrig. Sci. 31 (1), 27–36. https://doi.org/10.1007/s00271-011-0289-x.

Dabach, C., Shani, U., Lazarovitch, N., 2015. Optimal tensiometer placement for high-frequency subsurface drip irrigation management in heterogeneous soils. Agric. Water Manag. 152, 91–98 2015.

Ebrahimian, H., Liaghat, A., Parsinejad, M., Abbasi, F., Navabian, M., 2012. Comparison of one- and two- dimensional models to simulate alternate and conventional furrow fertigation. J. Irrig. Drainage Eng. 138 (10), 929–938. https://doi.org/10.1061/(ASCE)IR.1943-4774.0000482.

Ebrahimian, H., Liaghat, A., Parsinejad, M., Playan, E., Abbasi, F., Navabian, M., 2013a. Simulation of 1D surface and 2D subsurface water flow and nitrate transport in alternate and conventional furrow fertigation. Irrig. Sci. 31, 301–316. https://doi.org/10.1007/s00271-011-0303-3.

Ebrahimian, H., Liaghat, A., Parsinejad, M., Playan, E., Abbasi, F., Navabian, M., Lattore, B., 2013b. Optimum design of alternate and conventional furrow fertigation to minimize nitrate loss. J. Irrig. Drainage Eng. 139 (11), 911–921. https://doi.org/10.1061/(ASCE)IR.1943-4774.0000635.

Feddes, R.A., Kowalik, P.J., Zaradny, H., 1978. Simulation of Field Water Use and Crop Yield. John Wiley & Sons, New York, NY.

Hamlett, J.M., Baker, J.L., Horton, R., 1990. Water and anion movement under ridge tillage: a field study. Trans. ASAE 33, 1859–1866.

Hanson, B.R., Šimůnek, J., Hopmans, J.W., 2006. Numerical modeling of urea-

ammonium-nitrate fertigation with drip irrigation using numerical modeling. Agric. Water Manag. 86, 102–113.
Kemper, W.D., Olsen, J., Hodgdon, A., 1975. Fertilizer or salt leaching as affected by subsurface shaping and placement of fertilizer and water. Proceed. Soil Sci. Soc. Am. 39, 115–119.
Klocke, N.L., Schneekloth, J.P., Melvin, S., Clark, R.T., Payero, J.O., 2004. Field scale limited irrigation scenarios for water policy strategies. Appl. Eng. Agric. 20, 623–631.
Lazarovitch, N., Warrick, A.W., Furman, A., Zerihun, D., 2009. Subsurface water distribution from furrows described by moment analyses. J. Irrig. Drain. Eng. 135 (1), 7–12.
Li, Y., Šimůnek, J., Zhang, Z., Jing, L., Ni, L., 2015. Evaluation of nitrogen balance in a direct-seeded-rice field experiment using Hydrus-1D. Agric. Water Manag. 148, 213–222. https://doi.org/10.1016/j.agwat.2014.10.010.
Liu, K., Huang, G., Xu, X., Xiong, Y., Huang, Q., Šimůnek, J., 2019. A coupled model for simulating water flow and solute transport in furrow irrigation. Agric. Water Manag. 213, 792–802.
Mailhol, J.C., Ruelle, P., Nemeth, I., 2001. Impact of fertilisation practices on nitrogen leaching under irrigation. Irrig. Sci. 20, 139–147.
Mailhol, J.C., Crevoisier, D., Triki, K., 2007. Impact of water application conditions on nitrogen leaching under furrow irrigation: experimental and modeling approaches. Agric. Water Manag. 87 (3), 275–284.
Oster, J.D., Letey, J., Vaughan, P., Wu, L., Qadir, M., 2012. Comparison of transient state models that include salinity and matric stress effects on plant yield. Agric. Water Manag. 103, 167–175.
Payero, J.O., Melvin, S.R., Irmak, S., Tarkalson, D., 2006. Yield response of corn to deficit irrigation in a semiarid climate. Agric.Water Manage 84, 101–112.
Pratt, P.F., Jury, W.A., 1984. Pollution of the unsaturated zone with nitrate. In: In: Yaron, B., Dagan, G., Goldshmid, J. (Eds.), Pollutants in Porous Media. Ecological Studies (Analysis and Synthesis) 47 Springer, Berlin, Heidelberg.
Ragab, R., Battilani, A., Matovic, G., Stikic, R., Psarras, G., Chartzoulakis, K., 2015. SALTMED model as an integrated management tool for water, crop, soil and N-fertilizer water management strategies and productivity: field and simulation study. Irrig. Drain. 64, 13–28.
Ramos, T.B., Šimůnek, J., Gonçalves, M.C., Martins, J.C., Prazeres, A., Pereira, L.S., 2012. Two-dimensional modeling of water and nitrogen fate from sweet sorghum irrigated with fresh and blended saline waters. Agric. Water Manag. 111, 87–104. https://doi.org/10.1016/j.agwat.2012.05.007.
Rocha, D., Abbasi, F., Feyen, J., 2006. Sensitivity analysis of soil hydraulic properties on subsurface water flow in furrows. J. Irrig. Drain. Eng. 132 (4), 418–424.
Šimůnek, J., Hopmans, J.W., 2009. Modeling compensated root water and nutrient uptake. Ecol. Model. 220 (4), 505–521. https://doi.org/10.1016/j.ecolmodel.2008.11.004.
Šimůnek, J., van Genuchten, M.T., Šejna, M., 2008. Development and applications of the HYDRUS and STANMOD software packages and related codes. Vadose Zone J. 7 (2), 587–600. https://doi.org/10.2136/VZJ2007.0077.
Šimůnek, J., Bristow, K.L., Helalia, S.A., Siyal, A.A., 2016a. The effect of different fertigation strategies and furrow surface treatments on plant water and nitrogen use. Irrig. Sci. 34 (1), 53–69. https://doi.org/10.1007/s00271-015-0487-z.
Šimůnek, J., van Genuchten, M.T., Šejna, M., 2016b. Recent developments and applications of the HYDRUS computer software packages. Vadose Zone J. 15 (7), 25. https://doi.org/10.2136/vzj2016.04.0033.
Siyal, A.A., Bristow, K.L., Šimůnek, J., 2012. Minimizing nitrogen leaching from furrow irrigation through novel fertilizer placement and soil management strategies. Agric. Water Manag. 115, 242–251.
Soroush, F., Mostafazadeh-Fard, B., Mousavi, S.F., Abbasi, F., 2012. Solute distribution uniformity and fertilizer losses under meandering and standard furrow irrigation methods. Aust. J. Crop Sci. 6 (5), 884–890.
Tiercelin, J.R., Vidal, A., 2006. Traite´ d'Irrigation, 2nd ed. Lavoisier, Technique and Documentation, Paris, France.
van Genuchten, M.Th., 1980. A closed-form equation for predicting the hydraulic conductivity of unsaturated soils. Soil Sci. Soc. Am. J. 44, 892–898.
Vrugt, J.A., Hopmans, J.W., Šimůnek, J., 2001. Calibration of a two-dimensional root water uptake model. Soil Sci. Soc. Am. J. 65 (4), 1027–1037.
Vrugt, J.A., van Wijk, M.T., Hopmans, J.W., Šimůnek, J., 2002. One-, two-, and three-dimensional root water uptake functions for transient modeling. Water Resour. Res. 37 (10), 2457–2470.
Waddell, J.T., Weil, R.R., 2006. Effect of fertilizer placement on solute leaching under ridge tillage and no till. Soil Tillage Res. 90, 194–204.
Walker, W.R., Skogerboe, G.V., 1987. Surface Irrigation: Theory and Practice. Prentice-Hall Inc., Englewood Cliffs, New Jersey 386 p.
Warrick, A.W., Lazarovitch, N., Furman, A., Zerihun, D., 2007. Explicit infiltration function for furrows. J. Irrig. Drain. Eng. 133 (4), 307–313.
Wöhling, T., Mailhol, J.C., 2007. A physically based coupled model for simulating 1D surface - 2D subsurface flow and plant water uptake in irrigation furrows. II: model test and evaluation. J. Irrig. Drain. Eng. 133 (6), 548–558.
Wöhling, T., Schmitz, G.H., 2007. A physically based coupled model for simulating 1D surface - 2D subsurface flow and plant water uptake in irrigation furrows. I: model development. J. Irrig. Drain. Eng. 133 (6), 538–547.
Wöhling, T., Schmitz, G.H., Mailhol, J.C., 2004a. Modeling two-dimensional infiltration from irrigation furrows. J. Irrig. Drain. Eng. 130 (4), 296–303.
Wöhling, T., Singh, R., Schmitz, G.H., 2004b. Physically based modeling of interacting surface–subsurface flow during furrow irrigation advance. J. Irrig. Drain. Eng. 130 (5), 349–356.
Wöhling, T., Fröhner, A., Schmitz, G.H., Liedl, R., 2006. Efficient solution of the coupled one-dimensional surface - two-dimensional subsurface flow during furrow irrigation advance. J. Irrig. Drain. Eng. 132 (4), 380–388.
Zerihun, D., Sanchez, C.A., Lazarovitch, N., Warrick, A.W., Clemmens, A.J., Bautista, E., 2014. Modeling flow and solute transport in irrigation furrows. Irrig. Drain. Syst. Eng. 3 (2), 16. https://doi.org/10.4172/2168-9768.1000124. 124.